

## **Image-based detection and analysis of crack propagation in cementitious composites**

E.B. Pereira<sup>1</sup>, G. Fischer<sup>2</sup>, and J.A.O. Barros<sup>3</sup>

<sup>1</sup> *ISISE, University of Minho, Guimaraes, Portugal*

<sup>2</sup> *Technical University of Denmark, Lyngby, Denmark*

<sup>3</sup> *ISISE, University of Minho, Guimaraes, Portugal*

The initiation and propagation of cracking in concrete and other cementitious materials is a governing mechanism for many physical and mechanical material properties. The observation of these cracking processes in concrete is typically taking place at discrete locations using destructive methods after the cracking process has occurred. The alternative non-destructive methods are often either not precise enough or experimentally too demanding. In this study, the use of an image analysis procedure to capture the crack initiation and propagation process is described, which utilizes digital images of the concrete surface while undergoing the cracking process. The results obtained with this method have shown that it is possible to monitor relatively small displacements on the specimen surface independently of the scale of the representative area of interest. The formed cracks are visible at relatively small crack openings, allowing a thorough investigation and analysis of the cracking processes in concrete.

Corresponding author's email: [eduardo.pereira@civil.uminho.pt](mailto:eduardo.pereira@civil.uminho.pt)

# Image-based detection and analysis of crack propagation in cementitious composites

E.B. Pereira<sup>1</sup>, G. Fischer<sup>2</sup>, and J.A.O. Barros<sup>3</sup>

<sup>1</sup> ISISE, University of Minho, Guimaraes, Portugal

<sup>2</sup> Technical University of Denmark, Lyngby, Denmark

<sup>3</sup> ISISE, University of Minho, Guimaraes, Portugal

**ABSTRACT:** The initiation and propagation of cracking in concrete and other cementitious materials is a governing mechanism for many physical and mechanical material properties. The observation of these cracking processes in concrete is typically taking place at discrete locations using destructive methods after the cracking process has occurred. The alternative non-destructive methods are often either not precise enough or experimentally too demanding. In this study, the use of an image analysis procedure to capture the crack initiation and propagation process is described, which utilizes digital images of the concrete while undergoing the cracking process. The results obtained with this method have shown that it is possible to monitor relatively small displacements on the specimen surface independently of the scale of the representative area of interest. The formed cracks are visible at relatively small crack openings, allowing a thorough investigation and analysis of the cracking processes in concrete.

## 1 INTRODUCTION

The mechanical properties of concrete are very closely related to the formation of cracks. The macroscopic aspects of the mechanical and physical behavior of concrete stem from its intrinsic cracking mechanisms. Due to their importance, the initiation and the propagation of cracks in concrete and other cement based composites have been studied extensively in the past few decades. The moderate strain hardening prior to the attainment of the ultimate tensile capacity and the subsequent rapid strain softening constitute the quasi-brittle mechanical behavior typical of concrete. Classic linear elastic fracture mechanics (LEFM) was found to be insufficient for the complete characterization of this quasi-brittle behavior. The so-called cohesive crack concept has emerged to complement LEFM, which relies on the existence of a diffusely micro-cracked region ahead of the macro-crack. The transition zone between the intact material and the fully developed macro-crack still exhibits some residual stress transfer ability. All the relevant micro-cracking mechanisms, which lead to the type of material behavior commonly associated with concrete seem to be located in this region, also known as the fracture process zone (FPZ) (Karihaloo et al. 1993; Landis and Shah 1995; Wittmann and Xiaozhi H 1991).

Research has been carried out extensively over the past two decades towards a better understanding of the FPZ. The particularly complex nature of the cracking processes in concrete demands for special techniques of analysis and the very fine cracks to be detected require high resolution equipment for image capturing and analysis (Hornain et al. 1996, Otsuka and Date 2000). In addition, most of the intrusive characterization techniques used in other materials may

produce preliminary cracks in concrete, either due to the direct mechanical action, induced drying or the alteration of other physical variables important for the delicate balance of the microstructure of concrete. Many different techniques have been specially developed for the analysis of FPZ and cracking in concrete and other cement based materials. Radiography (x-rays, neutrons, or others), impregnation, acoustic emission, ultrasound, laser holography and interferometry represent some of the techniques that have successfully revealed quantitative information about the FPZ (He et al. 1995; Knab et al. 1984; Landis et al. 2007; Otsuka and Date 2000; Regnault and Brühwiler 1990; Shah 1990). Although most of the macroscopic features of cracking processes in concrete are well understood, the micro-mechanisms of cracking and the essence of FPZ still maintain some uncertainties. More quantitative and qualitative information about the FPZ is still required, as it can help to improve the design of cement based materials and in particular the design of more efficient fiber reinforced cementitious composites (FRCC).

With the recent developments of the digital photography technology, the relevance of digital acquisition of images in scientific research has increased. Charged couple devices (CCD) have reached levels of resolution and quality that allow the image-based documentation of small scale cracking processes. In particular, a non-contact full-field strain measuring technique has been developed to obtain full field surface displacements and strains of objects under load. The so-called Digital Image Correlation (DIC) involves the comparison of two digitized images of the surface of an object before and after deformation using an appropriate correlation technique (Chu et al. 1995). The efficiency and reliability of this method have evolved over the last decade with the vast improvements of the computations, algorithms and imaging technologies. Applications of DIC exist for the examination of deformations of distinct materials at different scales (Abanto-Bueno and Lambros 2005; Corr et al. 2007; Savic et al. 2010; Yomeyama et al. 2006). The method is not limited by an intrinsic length scale, which makes it very attractive for use over multiple length scales. The accuracy of the correlation between recorded images depends upon the quality of the image speckle pattern (including light conditions) and the resolution of the imaging system (Berfield et al. 2007).

The powerful full-field image-based monitoring of the surface displacements of concrete specimens under tensile stresses is expected to reveal relevant details about propagating cracks. The observation of the surface displacements in concrete specimens under controlled tensile loading conditions and near crack tip regions may allow the detection and follow up of a crack, from its initiation to its fully open state. This is possible for crack stages where the crack is still far from becoming visible or detectable by conventional means. Relevant information about toughening mechanisms and phase interaction in cement based materials may be added in future work, with a positive impact on the understanding of the tensile micro-mechanisms taking place during cracking.

## 2 EXPERIMENTAL PROCEDURE

The testing procedure developed for the present work consisted of applying a tensile load to a single-edge notched specimen. The specimen shape adopted resembles the one used for the evaluation of the crack growth behavior in metals (ASTM-E647 2005), the so-called Compact Tension (CT) specimen. Clear access to the surface where the crack progression becomes visible is important. At the same time, the stress intensity achieved at the tip of the notch limits the area where the crack initiates. With the purpose of maximizing the stress intensity at the tip of the notch, the notch thickness was minimized to 0.5 mm using a small diamond cutting disc. The depth of the specimen was also minimized, promoting the plain stress state. Summarizing, the dimensions adopted for the specimens were 150 mm (perpendicular to the notch) by 125 mm (parallel to the notch) and 12 mm (thickness). The available path for the initiated crack to progress parallel to the notch was 45 mm. The distance between the loading axis and the tip of the notch was also 45 mm (Figure 1).

The testing sequence consisted of imposing the specimens to a tensile load at a constant displacement rate, transmitted by two rods with a diameter of 22 mm (see Figure 2). The use of the two rods allowed the transmission of the displacement while keeping free the rotation of the specimen with respect to the rods. The displacement rate adopted was 5  $\mu\text{m/s}$ .

Four specimens with different compositions were tested: cement paste, mortar, concrete and FRCC. The composition of the cement paste was cement and water only. The composition of the concrete was cement, water and aggregates with a maximum size of 4 mm. The composition of the mortar was cement, fly ash, fine sand (0.170 mm) water and admixtures. The FRCC was composed of cement, fly ash, fine sand (0.170 mm), water, admixtures and Polyvinyl Alcohol (PVA) fibers.

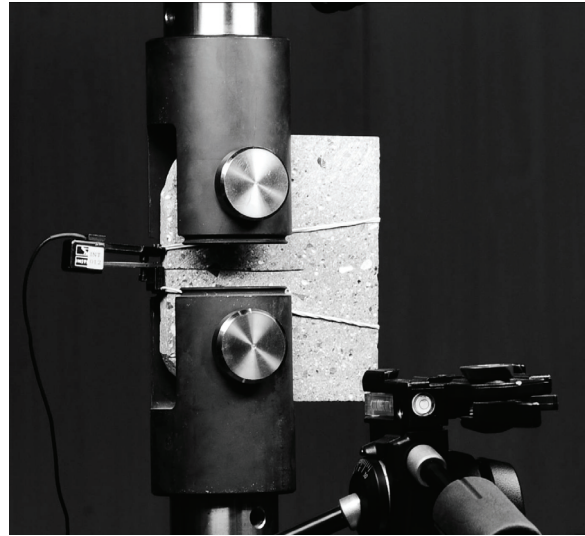
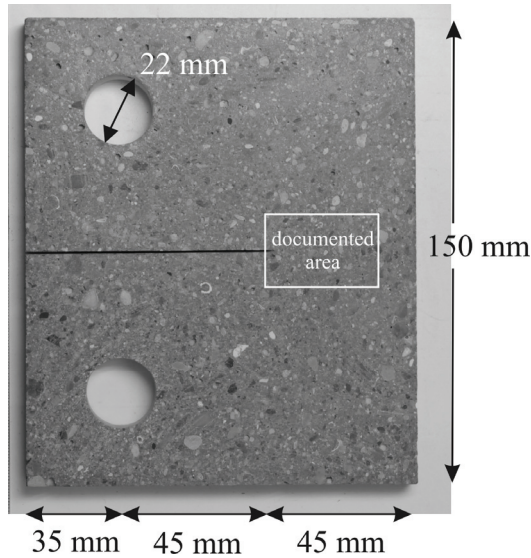


Figure 1. Specimen geometry for the CT test.

Figure 2. CT test setup.

The formation and propagation of the tensile crack was traced on the surface of the specimens using a high resolution digital camera, positioned 90 mm away from the specimen. The 60 mm focal length lens allowed the observation of a 36 mm by 36 mm area of the surface of the specimen (see Figure 1). Images with 24 megapixel of resolution were captured during testing with time intervals of one second. These images were subsequently used for the continuous interpolation of the strain fields at the inspected surface of the specimen.

The optimal conditions for the strain field interpolation were met without the need of applying a speckle pattern on the surface of the specimen (see Figure 3 and Figure 4). Sufficient randomness and high contrast of the stochastic patterns captured from the surface are important for the continuous recognition and tracing of the shape and position of each facet (Berfield et al. 2007). In the present case, fluorescent lights were used and positioned in such a way that the light intensity reflected by the specimen surface was even. The images of the surface of the specimens were analyzed prior to testing and sufficient image correlation was obtained. Each facet was composed of  $15 \times 15$  pixels. Each pixel covered a real area of  $6 \times 6 \mu\text{m}^2$ . The total area of  $36 \times 36 \text{ mm}^2$  was modeled by a facet mesh overlay composed of approximately  $400 \times 260$  facets.

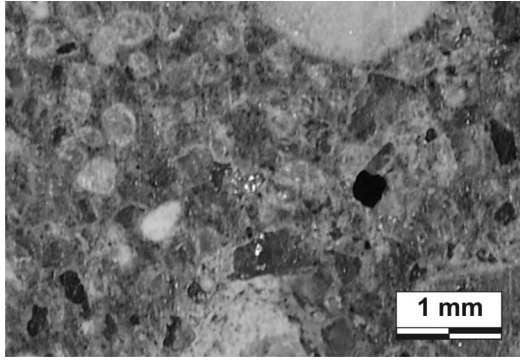


Figure 3. Amplified image captured from the surface of the concrete specimen.

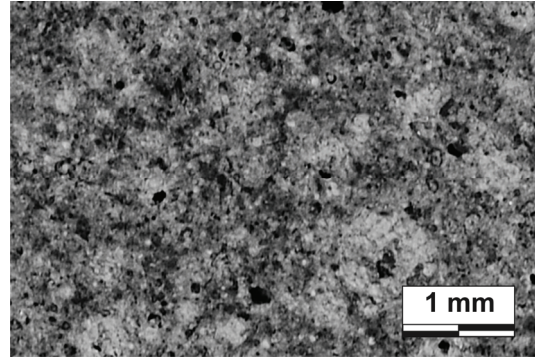


Figure 4. Amplified image captured from the surface of the mortar specimen.

### 3 RESULTS AND DISCUSSION

The results obtained in terms of load – crack mouth opening displacement (CMOD) during testing are presented in Figure 5. The CMOD was measured using a clip gage, positioned at the edge of the notch (Figure 2). The results are presented for CMOD values of up to 1.6 mm.

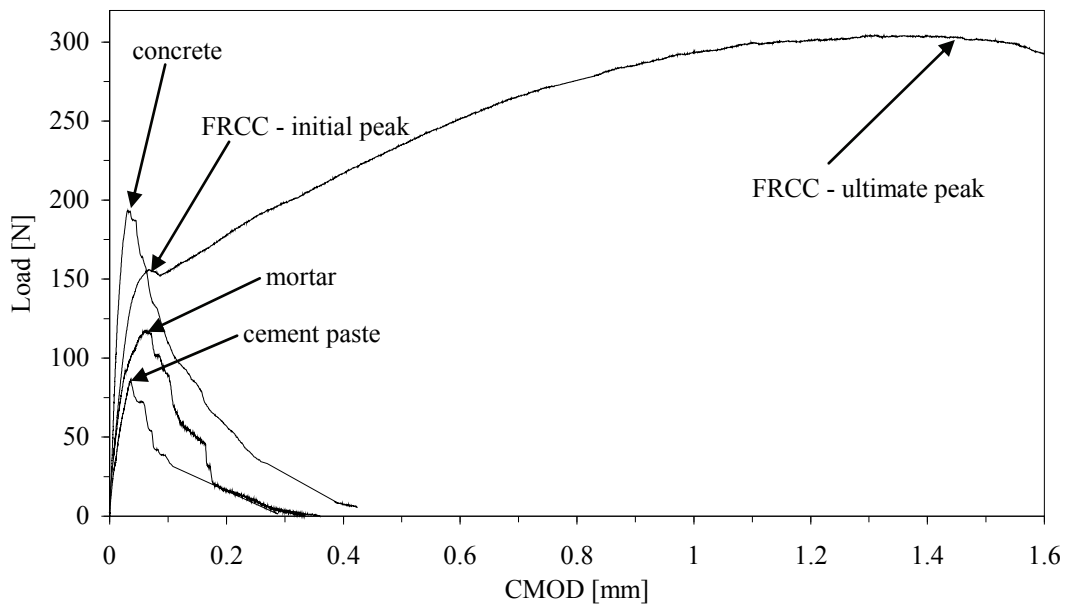


Figure 5. Load – CMOD curves measured during testing. The peak loads are identified for all specimens

In general, the load-CMOD curves obtained for the three non-reinforced cementitious matrices present a similar shape. The registered behavior is quasi-brittle, showing the typical moderate tensile hardening before reaching the peak load and the subsequent rapid strain softening. The cement paste reached the lowest tensile load (86 N), and the concrete the highest (192 N). The post-peak softening branch in the concrete specimen was smoother than in the other two unreinforced cementitious matrices. The presence of aggregates seemed to help with the development of a more controlled fracture process, minimizing the sudden energy release events and corresponding abrupt load drops during softening. The existence of the PVA fibers in the FRCC specimen caused a pronounced second tensile strain hardening stage after the first peak load (initial peak). In the FRCC specimen, the maximum tensile load of 304 N was reached at a CMOD of 1.46 mm (global peak).

The shape of the crack obtained in each specimen during testing is shown in Figure 6. These cracks are generally straight and show no evident signs of smearing or branching. They initiate at the tip of the notch and propagate to the edge of the specimen by following the shortest path.

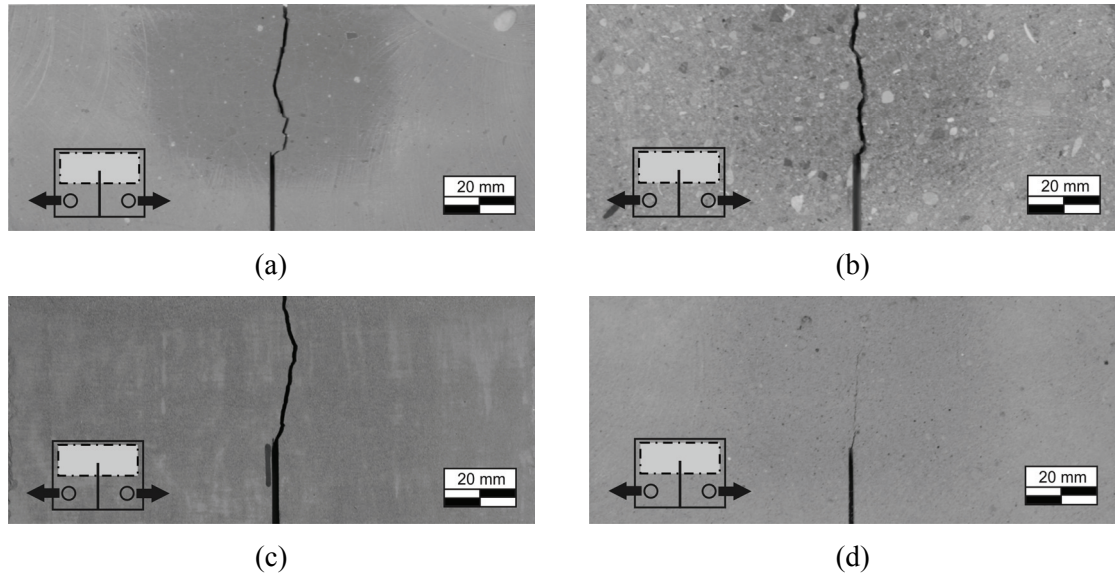


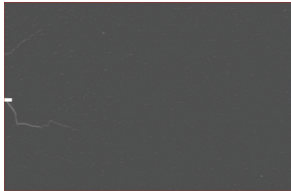
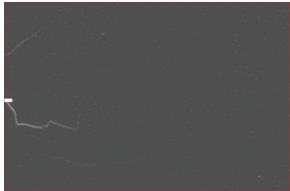
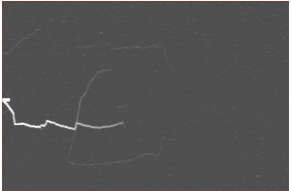

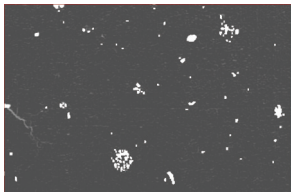
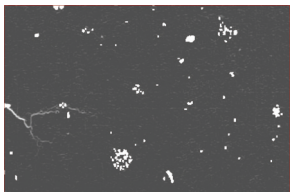
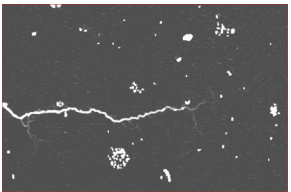

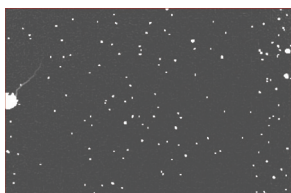
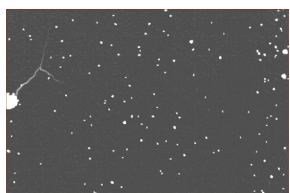
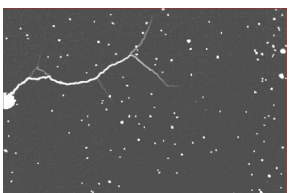





Figure 6. Images of the cracks formed in each specimen: (a) cement paste, (b) concrete, (c) mortar and (d) FRCC.

In Table 1 the results obtained with the image-based monitoring system are shown. The maximum principal strains derived from the interpolated displacement fields at the facets overlay are represented. The color gradient evolves from dark grey (zero strain) to white (maximum strain of 5%). These strain values refer to the displacement gradients derived at the facets overlay. A discrete displacement jump between the two opposite crack faces is revealed by a strong strain gradient registered in the facets traversed by the crack. These strains are physically not realistic, in the sense that they result from the smearing of the local displacement jump occurring between the crack faces by the traversed facets using the principles of linear elasticity (Chu et al. 1985). Despite this unusual representation of a crack opening with strain, the results visualize well the extent of cracking.

The sequence of pictures taken with a time interval of one second allowed the reconstruction and tracing of the full field displacements and strains during the entire testing procedure. To illustrate the obtained results, three representative stages were selected: before the peak load was reached (90% of the peak value), when the peak load was reached and after the peak load (50% of the peak value). In the case of the FRCC specimen, the peak load refers to the first peak load. The strong geometrical gradients found in larger pores and defects located at the imaged surface of the specimens influence the pattern correlation. As a consequence, some of the facets in the overlay show the white color, corresponding to areas where the image correlation failed. Additionally, when the pattern at the surface does not have enough contrast or randomness of the intrinsic features, the pattern correlation and facet recognition may also be unsatisfactory.

The images in Table 1 allow the observation of how the cracks initiate and propagate in each specimen. The cracks become clearly visible for very small openings. The opening values measured at the crack tip when 90% of the peak load is reached in the cement paste (4  $\mu\text{m}$ ), mortar (4  $\mu\text{m}$ ), concrete (5  $\mu\text{m}$ ) and FRCC (4  $\mu\text{m}$ ) specimens are small. The images presented in Table 1 are amplified for the mortar, concrete and FRCC specimens near the notch tip for this stage (Figure 7). The technique revealed high potential for detecting very small cracks when compared to alternative methods.

Table 1. Sequence of frames showing the maximum principal strains observed in the facet overlay for three different load levels: before the peak load (90% of the peak load); when the peak load is reached; after the peak load (50% of the peak load).

|                 | 90% of peak load<br>(before peak)   | peak load   | 50% of peak load<br>(after peak)   |   |
|-----------------|---|---|--|---|
| Cement<br>paste |    |    |    |    |
| concrete        |    |    |    |    |
| mortar          |    |    |    |    |
| FRCC            |  |  |  |  |

In general, for all specimens the measured deformations reveal the initiation of the cracks at the tip of the notch at very early stages. The progression of these cracks was followed very precisely afterwards. In some cases, the main crack diverted from its main horizontal path to which it returned later on, leaving behind a crack branch. This behavior becomes particularly clear in the mortar specimen, where long branches of the main crack were detected. These branches were untraceable in the final cracked specimens. What seemed to be a single crack in the final cracked specimens turned out to be in fact the final path which prevailed among a number of cracking branches and crack path diversions.

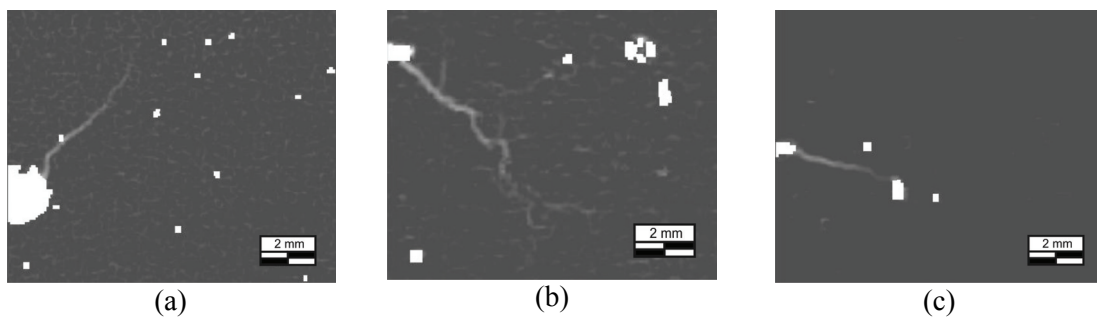


Figure 7. Images amplified near the notch tip, corresponding to the stage when 90% of the peak load was reached: (a) mortar, (b) concrete and (c) FRCC (first peak).

Considering the results obtained from the cement paste specimen (Table 1), secondary cracks become visible right from the onset of the testing sequence, even at low load levels. These secondary cracks were not connected to the principal crack initiating at the notch tip. They become visible with the increase of the tensile stress in the vicinity. Therefore, these are probably shrinkage cracks that become active when the specimen is loaded. Given that the cement paste specimen is made of cement and water only, significant autogenous shrinkage can be expected. Ultimately, the crack path seems to be greatly influenced by these pre-existing shrinkage cracks, which divert the crack originated at the notch tip from its natural path. This explains the tortuous shape of the final crack and may also explain the lower initial stiffness observed in the load-CMOD diagram of the cement specimen.

The effect of crack branching is visible in all the specimens tested. However they assume different features. In the mortar specimen the crack branches developed are fewer, longer and discrete. In the concrete specimen the crack branching occurs more frequently and the branched cracks are less visible, apparently more diffuse and tortuous. A small area of diffuse micro-cracking ahead of the principal crack is visible in some stages too (Figure 7.b). The increase of the number of aggregates and their size contributed for the local intensification of crack smearing at the tip. At the same time, the crack branches become smaller and more frequent, suggesting that the smearing of the crack contributes for its arrestment and for the gradual release of the fracture energy. In the FRCC specimen branching and crack smearing are both less visible, for what the effect of the fibers may have contributed, by arresting the propagation of the micro-cracks.

#### 4 CONCLUSIONS

An intuitive analysis of the micro-cracking mechanisms occurring in cementitious composites was made possible by the image-based monitoring technique presented in this study. The full-field displacements interpolation and measurement at the surface of the specimens allowed the immediate interpretation of the micromechanical events taking place during the initiation and the propagation of the cracks. The effect of pre-existing cracks or other micro-defects, of fibers or aggregates, could be evaluated in a meticulous and efficient manner with the aid of the present technique.

The revealed cracking features were important for a better understanding of the mechanical test results. The influence of shrinkage induced pre-existing cracks on the final path of the principal crack was revealed by the images of the cement paste specimen. The secondary cracks detected with the increase of the load diverted and shaped the primary crack originated at the tip of the notch. At the same time, the presence of these pre-existing cracks contributed to explain the smaller initial stiffness registered for the cement past specimen. Similarly, the presence of different quantities of aggregates and with different sizes has influenced the morphology of the propagating cracks in the remaining specimens, especially near the crack tip. The cracks propagating in the cementitious composites containing less and smaller aggregates have revealed shorter and more smeared crack branches. In the FRCC specimen the crack branches were less visible, suggesting that the fibers have contributed effectively for the micro-cracking arrestment.

#### ACKNOWLEDGMENTS

The first author thanks the Portuguese National Science Foundation for the financial support, through grant SFRH / BD / 36515 / 2007, funded by POPH - QREN, the Social European Fund and the MCTES, and DTU-Byg for their support of the work as part of this project.



## REFERENCES

- Abanto-Bueno J., Lambros J. (2005) "Experimental determination of cohesive failure properties of a photodegradable copolymer". *Exp. Mech.* 45(2): 144-152.
- ASTM-E647 (2005) "Standard test method for measurement of fatigue crack growth rates". *ASTM Standards* Vol. 03.01, US.
- Berfield T.A., Patel J.K., Shimmin R.G., Braun P.V., Lambros J., Sottos N.R. (2007) "Micro- and nanoscale deformation measurement of surface and internal planes via digital image correlation". *Exp. Mech.* 47: 51-62.
- Chu T.C., Ranson W.F., Sutton M.A., Peters W.H. (1985) "Applications of digital-image-correlation techniques to experimental mechanics". *Exp. Mech.* 25(3): 232-244.
- Corr D., Accardi M., Graham-Brady L., Shah S. (2007) "Digital image correlation analysis of interfacial debonding properties and fracture behavior in concrete". *Eng. Fract. Mech.* 74: 109-121.
- He S., Feng Z., Rowlands R.E. (1995) "Fracture Process Zone Analysis of Concrete Using Moiré Interferometry". *Exp. Mech.* 37(3):367-373.
- Hornain H., Marchand J., Ammouche A., Commène J.P., Moranville M. (1996) "Microscopic observation of cracks in concrete – a new sample preparation technique using dye impregnation". *Cement Concrete Res.* 26(4): 573-583.
- Karihaloo B.L., Carpinteri A., Elices M. (1993) "Fracture mechanics of cement mortar and plain concrete". *Adv. Cem. Based Mater.* 1:92-105.
- Knab L.I., Walker H.N., Clifton J.R., Fuller Jr. E.R. (1984) "Fluorescent thin sections to observe the fracture zone in mortar". *Cement Concrete Res.* 14: 339-344.
- Landis E.N., Shah S.P. (1995) "The influence of micro-cracking on the mechanical behavior of cement based materials". *Adv. Cem. Based Mater.* 2: 105-118.
- Landis E.N., Zhang T., Nagy E.N., Nagy G., Franklin W.R. (2007) "Cracking, damage and fracture in four dimensions". *Mater. Struct.* 40:357-364.
- Otsuka K., Date H. (2000) "Fracture process zone in concrete tension specimen". *Eng. Fract. Mech.* 65: 111-131.
- Regnault PH., Brühwiler E. (1990) "Holographic interferometry for the determination of fracture process zone in concrete". *Eng. Fract. Mech.* 35:29-38.
- Sanford, R.J. (2003) "Principles of fracture mechanics". Prentice Hall, US.
- Shah S.P. (1990) "Experimental methods for determining fracture process zone and fracture parameters". *Eng. Fract. Mech.* 35:3-14.
- Savic V., Hector Jr L.G., Fekete J.R. (2010) "Digital image correlation study of plastic deformation and fracture in fully martensitic steels". *Exp. Mech.* 50: 99-110.
- Wittmann F.H., Xiaozhi H. (1991) "Fracture process zone in cementitious materials". *Int J Fracture* 51: 3-18.
- Yoneyama S., Morimoto Y., Takashi M. (2006) "Automatic evaluation of mixed-mode stress intensity factors utilizing digital image correlation". *Strain* 42: 21-29.